university of groningen

University Medical Center Groningen

University of Groningen

Free volume properties of a simulated lipid membrane

Marrink, S. J.; Sok, R. M.; Berendsen, H. J. C.

Published in:
Journal of Chemical Physics

DOI:
10.1063/1.471442

IMPORTANT NOTE: You are advised to consult the publisher's version (publisher's PDF) if you wish to cite from it. Please check the document version below.

Document Version
Publisher's PDF, also known as Version of record

Publication date:
1996

Link to publication in University of Groningen/UMCG research database

Citation for published version (APA):
Marrink, S. J., Sok, R. M., & Berendsen, H. J. C. (1996). Free volume properties of a simulated lipid membrane. *Journal of Chemical Physics*, *104*(22), 9090 - 9099. https://doi.org/10.1063/1.471442

Copyright
Other than for strictly personal use, it is not permitted to download or to forward/distribute the text or part of it without the consent of the author(s) and/or copyright holder(s), unless the work is under an open content license (like Creative Commons).

The publication may also be distributed here under the terms of Article 25fa of the Dutch Copyright Act, indicated by the "Taverne" license. More information can be found on the University of Groningen website: https://www.rug.nl/library/open-access/self-archiving-pure/taverne-amendment.

Take-down policy
If you believe that this document breaches copyright please contact us providing details, and we will remove access to the work immediately and investigate your claim.

Downloaded from the University of Groningen/UMCG research database (Pure): http://www.rug.nl/research/portal. For technical reasons the number of authors shown on this cover page is limited to 10 maximum.

Download date: 04-05-2023

Free volume properties of a simulated lipid membrane

S. J. Marrink
Biophysical Chemistry, University of Groningen, Nijenborgh 4, 9747 AG Groningen, The Netherlands

R. M. Sok
BASF-AG Ludwigshaven, ZX/ZC-C13, 67056 Ludwigshaven, Germany

H. J. C. Berendsen
Biophysical Chemistry, University of Groningen, Nijenborgh 4, 9747 AG Groningen, The Netherlands

(Received 4 August 1995; accepted 7 March 1996)

In this paper, an extensive analysis of free volume related properties of a lipid membrane is given. Using percolation theory, and comparing the free volume properties to those of a soft polymer, additional insights are obtained. The analyses are discussed within the framework of the four region model. It is concluded that the four regions have very different free volume properties. The region containing the dense part of the lipid tails resembles a soft polymer membrane to a large extent. The middle part of the membrane is more similar to a low density alkane. The consequences of the computed free volume properties on the permeation process of small penetrants are discussed. © *1996 American Institute of Physics.* [S0021-9606(96)50922-0]

I. INTRODUCTION

In a previous study,[1] we analyzed molecular dynamics (MD) simulations of a lipid membrane and showed that the properties are representative for a liquid-crystalline membrane. This study is completely concerned with the analyses of free volume properties of the lipid membrane, using the same simulation data. Apart from a general interest in membrane properties, free volume properties are of particular importance to the permeation process of small molecules. Therefore, this study forms the basis of an extended study of the permeation process of small molecules across a lipid membrane, which has already been initiated with the study of the permeation process of water.[2]

We will study the free volume properties of the lipid membrane in the context of percolation theory. Since the membrane is inhomogeneous, the different regions of the membrane behave rather differently considering their free volume properties. Percolation theory offers a solid basis to understand those differences. We will also compare the free volume properties of the lipid membrane with other, simpler systems. An extensive comparison is made with the recent simulation of a soft polymer system.[3] This is of special importance as the permeation process of small particles across the lipid membrane is observed to resemble the permeation process across soft polymers.[4,5]

The free volume properties that we have analyzed are: *free volume fraction, percolation threshold, hole size distribution, asphericity parameter, and orientation parameter*. Each of these free volume properties are evaluated as a function of the position along the bilayer normal, and as function of penetrant size. The importance of these properties to the permeation process can be briefly summarized as follows. The *free volume fraction* is a direct measure of the amount of volume that is accessible to a certain penetrant molecule. We will explicitly look at the scaling properties of the free volume as a function of penetrant size. Many diffusion theories are directly related to free volume fractions. Obviously, small penetrants will have more free volume available than large ones, and therefore be able to diffuse faster. Also, the solvation free energy of the penetrant into the membrane will be strongly connected to the available free volume. The *percolation threshold* of a system indicates whether the free volume fraction is completely connected throughout the system or not. It is important for the free volume properties, since close to the percolation threshold different behavior is observed than away from it. The *hole size distribution* gives more specific information about how the available free volume is distributed, i.e., into many small holes or a few large ones. Free volume theories of a hopping type of diffusion process are often based on the distribution of penetrant accessible hole sizes. Finally, the *asphericity parameter* and the *orientation parameter* describe the shape and orientation of the free volume pockets in the membrane, which is of special importance to predict the effect of nonsphericity of the penetrant molecules on the permeation process.

The next section presents the basics of percolation theory, that we need in order to describe free volume properties of the membrane. Thereafter, the methods of analysis are described, followed by the presentation of the results and a discussion. The results are presented and discussed within the framework of a ''four region model.'' Finally, the main conclusions are summarized.

II. PERCOLATION THEORY

In the most general sense, percolation theory deals with the statistical aspects of multicomponent phases. These phases can consist of, for example, conducting and insulating components, oil and rock, or of atoms, and free volume as in our problem. In any case percolation theory can be used to understand large scale behavior independent of the details of the system, i.e., the same definitions and equations can be used to describe conducting properties in semi-insulators as well as free volume properties of lipid membranes. The as-

 0021-9606/96/104(22)/9090/10/$10.00 © 1996 American Institute of Physics

Downloaded¬13¬Nov¬2006¬to¬129.125.25.39.¬Redistribution¬subject¬to¬AIP¬license¬or¬copyright,¬see¬http://jcp.aip.org/jcp/copyright.jsp

pects of percolation theory that we will use in this study are summarized in this section. A more comprehensive treatment can be found in the literature.[6]

A. Percolation threshold

If the free volume of a specific system is connected from one side to the other side, the free volume is said to be *percolating*. The fraction of free volume p for which percolation occurs is called the percolation threshold, p_c. For larger fractions of free volume, almost all free volume will belong to the percolating cluster. For smaller fractions the free volume is disconnected into many smaller free volume clusters. Close to the percolation threshold many system properties show critical behavior characterized by scaling laws.

B. Hole size distribution

From now on, clusters of free volume will be called holes or pockets, which are more convenient terms considering the accessibility of penetrants in the membrane. The size (=volume) of such a hole is denoted as s. Percolation theory predicts that the hole size distribution $n(s,p)$ follows the following general formula:

$$n(s,p) \propto s^{-\tau} f(Z) \tag{1}$$

with

$$Z=(p-p_c)s^{\sigma} \tag{2}$$

and

$$\begin{aligned} f(Z) &\propto Z^{(\tau-\theta)/\sigma} \exp(-c|Z|^{1/\sigma}) \quad (Z<0) \\ &= C \quad (|Z|\to 0) \\ &\propto Z^{(\tau-\theta')/\sigma} \exp(-c' Z^{(1-1/d)/\sigma}) \quad (Z>0). \end{aligned} \tag{3}$$

In these expressions c, c', and C are constants, and d is the dimensionality. τ, σ, θ, and θ' are scaling exponents, which are believed to be universal (i.e., not dependent on details of the underlying system). Their estimated values in three dimensions are $\tau=2.18$, $\sigma=0.45$, $\theta=3/2$, and $\theta'=-1/9$. The parameter Z can be interpreted as a measure for the extent to which critical behavior is observed. In the limit of $|Z|\to 0$, critical behavior will be observed. The scaling function $f(Z)$ describes the transition from critical to noncritical behavior. The form of the scaling function can in general not be derived from theoretical considerations, and is based on computer experiments.

To understand the principles that govern the scaling behavior of the hole size distribution, it is easier to look at the various limits of Eq. (1). For systems for which $|Z|\to 0$, the scaling function will approach a constant, and a simple scaling law results:

$$n(s,p) \propto s^{-\tau} \quad (p \approx p_c \diagup s \to 0). \tag{4}$$

This limit applies to systems that are very close to the percolation threshold, or for very small hole sizes. In general, this scaling law is dominating the distribution of hole sizes up to the correlation length ξ of the system. This correlation length can be interpreted as an average distance of two free volume points belonging to the same cluster. At p_c, the correlation length becomes infinite, and the above scaling law remains valid over the whole range of hole sizes.

In the limit for large $|Z|$, Eq. (1) reduces to

$$\begin{aligned} n(s,p) &\propto s^{-\theta} \exp(-c''s) \quad (p<p_c \diagup s \to \infty) \\ &\propto s^{-\theta'} \exp(-c'''s^{1-1/d}) \quad (p>p_c \diagup s \to \infty). \end{aligned} \tag{5}$$

This equation applies to holes that are larger than the correlation length (which means to almost all hole sizes for systems that are not very close to the percolation threshold). Again, a power law is observed, but now with a different critical exponent. For very large holes, the exponential term becomes dominating. The crossover from power law to exponential decay not only depends on the size of the hole, but also on the deviation of the system from p_c, via the constants c'' and c'''. Systems that are further away from p_c will show power law behavior over a shorter range of hole sizes. For systems that are far from p_c, the hole size distribution will therefore be completely exponentially decaying.

C. Asphericity parameter

The asphericity parameter $a(s,p)$ is a measure for the ratio between the perimeter size s_{peri} and hole size s of the free volume pockets, and is defined as follows:

$$a(s,p)=\langle (4/3\pi)^{2/3} s_{\mathrm{peri}}/4\pi s^{2/3} \rangle_p . \tag{6}$$

The brackets denote an ensemble average at certain p. The prefactors originate from the ratio between perimeter and hole size for a perfect sphere, resulting in an asphericity parameter of 1 for a perfect sphere. Deviations from a perfect sphere shape will result in asphericity parameters larger than 1. For a cylindrically shaped hole, it is easy to derive that the asphericity parameter scales as

$$\begin{aligned} a &= (1+A)(\tfrac{3}{2}\sqrt{2}A)^{-2/3} \\ &\propto A^{1/3} \quad (A\to\infty), \end{aligned} \tag{7}$$

where A is the ratio between the long and short axis of the cylinder. For randomly shaped holes, the scaling behavior becomes more complicated, and will depend on the fractal dimension of the hole. For random percolation on a cubic lattice it can be shown that the perimeter size of very large holes becomes proportional to the hole size, implying an asphericity parameter proportional to the hole radius:

$$a(s,p) \propto s^{1/3}. \tag{8}$$

For small holes, however, the deformation into cylindrical shapes will dominate, and Eq. (7) can be applied to estimate the ratio of the principal axes.

D. Orientation parameter

Although the asphericity parameter gives information about the shape of the free volume pockets, it does not yield information about their orientation. Therefore, we define an orientation parameter $O(s,p)$ of a hole as the ratio between

Downloaded¬13¬Nov¬2006¬to¬129.125.25.39.¬Redistribution¬subject¬to¬AIP¬license¬or¬copyright,¬see¬http://jcp.aip.org/jcp/copyright.jsp

the radii of the hole in the directions perpendicular and lateral to the plane of the membrane. If this orientation parameter is larger than one, it means that the holes, on average, are oriented along the membrane normal, whereas an orientation parameter smaller than one means a preferential orientation along the membrane plane. Values close to 1.0 indicate an isotropic distribution. More sophisticated definitions are not necessary for the purpose of this research.

III. METHOD OF COMPUTATION

A. The membrane systems

The simulation of the lipid membrane system, consisting of 64 dipalmitoylphosphatidylcholine molecules (DPPC) and 736 water molecules, has been elaborately described elsewhere.[1] In short, this system has been simulated using the GROMOS[7] force field (with slight modifications[1]), under constant temperature (350 K) and constant pressure (1 atm) conditions. Periodic boundary conditions were applied in all directions. The free volume analyses presented in this work are based on the (well equilibrated) 80 ps trajectory of the membrane simulated in the liquid-crystalline state. Although the length of the analyzed trajectory is rather small, the calculated free volume properties are deduced to be statistically significant (see error discussion).

Part of the analyses that are performed for the lipid membrane, have also been performed on a soft polymer membrane.[8] The results will be used to compare with the membrane results. The soft polymer system consists of 12 chains of 60 dimethylsiloxane monomers, modeling polydimethylsiloxane (PDMS). The system was also simulated with the GROMOS simulation package for a period of 500 ps, with periodic boundary conditions applied in all directions. The details of the soft polymer simulation, including the forcefield, can be found elsewhere.[3]

B. Free volume

For the analysis of local free volume properties in the membrane, we wrote a general software package[9] that is able to compute various free volume related properties for a wide range of systems. The starting procedure of the free volume analysis program is the mapping of the system on a uniform grid. If a grid point lies within the van der Waals radius of one of the system atoms, it is denoted as occupied volume. If not, it is denoted as free volume. The fraction of free volume of the total volume is denoted as p. Considering penetrant diffusion in the membrane, it is important to distinguish two kinds of free volume. The first, which we will call *empty* free volume, V_{emp}, conforms to the definition given by Bondi,[10] and is computed as the fraction of grid points lying outside the van der Waals radii σ_i of any of the system atoms. The second one, the *accessible* free volume, V_{acc}, is calculated in the same way except for the addition of the van der Waals radius of the penetrant molecule, σ_j, to the radii of the system atoms. In the limiting case of a penetrant with zero radius, empty free volume and accessible free volume are equal.

In order to obtain local information on the free volume properties, i.e., a free volume distribution across the membrane, the free volume grid planes can be assigned to specific slices, for which the properties are averaged separately. The size of the grid was set to 100 grid points in the z direction. The lateral directions were scaled to ~80 grid points, according to their relative box lengths. Thus a grid density of approximately 1 point per 0.5 Å is obtained. Higher grid densities require too many computational efforts. Some test analyses performed with larger grids indicated no significant changes in the results.

C. Percolation threshold

For an infinite system the percolation threshold p_c is defined exactly as the free volume fraction for which percolation occurs. In finite systems (or semi-infinite systems, e.g., periodic systems such as the lipid membrane) this definition is not applicable, for two reasons. First, a finite system already percolates at a lower threshold as soon as the largest cluster reaches the system size. Besides, different samples of the same finite system will show different percolation thresholds. In order to get a good estimate of the real percolation threshold, several methods can be used.

To eliminate the first problem, the system size can be varied. From the scaling behavior of the apparent percolation threshold vs a large range of system sizes, the real percolation threshold can be deduced. However, the size of the membrane system is fixed, and can only be enlarged in the lateral direction. As we are interested in percolation behavior in the perpendicular direction only, we will compute apparent percolation thresholds only. Note that also a penetrant molecule will experience this apparent percolation threshold, instead of the real percolation threshold for an infinite system.

The second problem can be solved by using as many independent system samples (in our case: time frames) as possible. The percolation threshold can then be defined as the free volume fraction above which 50% of the samples percolates. Another definition involves the computation of the second moment of the hole size distribution (see below). If the percolating hole is disregarded, a maximum is observed at the percolation threshold.

D. Cluster analysis

The size of free volume holes in the free volume grid is calculated using a recursive algorithm. Starting at a grid point that is unoccupied, it looks at its (six) neighboring grid points, taking into account the periodicity of the system. If this neighboring grid point is also unoccupied, the algorithm looks at the neighbors of this grid point. This procedure is repeated until no more unoccupied neighbors are found. Each time that an unoccupied connected grid point is found, the size of the free volume hole is increased with 1. A percolating cluster is identified if the hole spans the system. This can happen in all three directions independently. Once all unoccupied grid points are assigned to a specific hole, the distribution of hole sizes $n(s,p)$ can be calculated. Assign-

Downloaded¬13¬Nov¬2006¬to¬129.125.25.39.¬Redistribution¬subject¬to¬AIP¬license¬or¬copyright,¬see¬http://jcp.aip.org/jcp/copyright.jsp

ing the geometric center of a hole to a particular slice in the membrane, the hole size distribution can also be obtained as a function of z, the position along the membrane normal.

Related to the hole size distribution is the cavity size distribution $n_{\mathrm{CAV}}(s)$. The probability density of a cavity large enough to accommodate a hard sphere of size between s and $s+ds$ is given by $n_{\mathrm{CAV}}(s)ds$, and is directly related to the accessible free volume: $n_{\mathrm{CAV}}(s)=-dV_{\mathrm{ACC}}(s)/ds$. Note that the cavity size distribution is not the same as the hole size distribution: a cavity of specific size s does not contain information about the volume of the associated free volume cluster, contrary to a hole of size s. The hole size distributions, which have to be evaluated for different penetrant sizes separately, yield more specific information.

The perimeter size of a hole, needed for the computation of the asphericity parameter, can be calculated together with the calculation of the hole size. The perimeter size is simply obtained by summing the number of occupied neighboring grid points of the hole (considering six possible neighbors per grid point). The radius of the hole in the lateral and perpendicular directions, needed for the computation of the orientation parameter, is also easily obtained once a hole is identified.

IV. RESULTS

A. Four region model

Based on both simulation results and on experimental data of various phospholipid membrane systems, we have previously[2,11] introduced a ''four region model.'' In this model, which is purely qualitative, the lipid membrane is divided into four different regions, each of these possessing some unique properties. Region 1 is the region in which the membrane headgroup density is still low, and is characterized mainly by loosely bound water molecules attached to choline headgroups. In region 2 the headgroup density is high, and the water molecules present in this region are strongly bound. It also contains the major part of the glycerol backbones. Region 3 contains the more ordered part of the lipid tails, with a density larger than liquid hexadecane. Region 4, finally, contains the major part of the lipid end groups. This region is much more disordered and therefore has a low density. Regions 1 and 2 are also referred to as the interface of the membrane, and regions 3 and 4 as the membrane interior. More details about the four region model can be found in the previous publications.[1,2,11]

In the forthcoming presentation and discussion of the results, we will make extensive use of this four region model in order to enhance the understanding of the free volume properties in different regions of the membrane.

B. Free volume

The most straightforward computation is the analysis of the average distribution of free volume that is accessible to a penetrant molecule. In Fig. 1, we plotted the accessible free volume expressed as fraction of the total volume for a series of differently sized, spherical penetrant molecules.

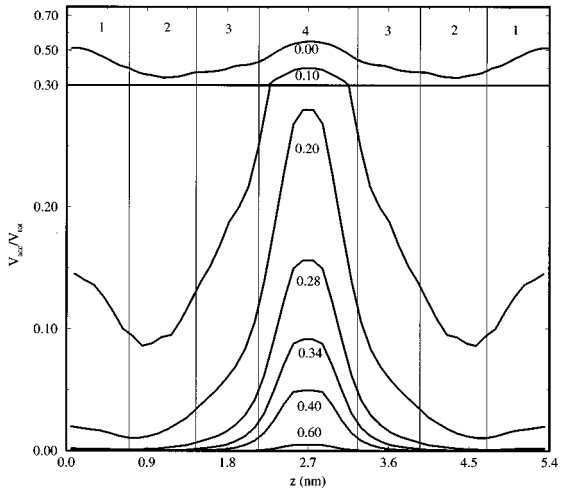

FIG. 1. Accessible free volume fraction p of differently sized penetrants, with diameters ranging from $\sigma=0.0$ (=empty free volume) to $\sigma=0.6$ nm. The middle of the water layer is located in region 1. Statistical errors in region 2 and 3 are ± 0.01, in the other regions less than 0.005.

The free volume distribution across the membrane is clearly far from homogeneous. The empty free volume distribution is complementary to the electron density distribution of this system.[1] This is obvious, as the free volume is defined to exist only in the absence of atom density. The empty free volume is lowest in region 2, due to the strong electrostatic attractions present between the lipid headgroups. As a consequence, the lipid tails in region 3 are also forced to pack densily, leaving not much free volume. The order parameter profile, as computed previously,[1] showed already that in this part of the membrane the tails are more neatly aligned parallel to each other and therefore can pack in a more efficient way. Towards the middle of the bilayer (region 4), the available free volume increases substantially. This is caused by the increase of the number of gauche angles which are more favored in the neighborhood of end groups. In addition, methyl groups pack with a lower density than methylene groups do.

Experimentally,[10] the empty free volume fraction in liquid hexadecane at 293 K is found to be 0.417. At the boiling point (559 K) this value is 0.565. Using a linear interpolation we estimated a value of 0.45 at the simulation temperature (350 K) which equals the calculated value of the membrane approximately halfway the lipid tails. The empty free volume fraction in region 3 is on average 0.40, which is close to the empty free volume fraction of 0.38 in the simulated soft polymer PDMS.

The largest accessible free volume is found in the middle of the membrane; even penetrant molecules with a diameter of 0.6 nm (e.g., urea) could fit on average into almost 1% of the total volume, without disturbing the surrounding lipids. For the smallest penetrants, like water, oxygen, and ammonia, with a diameter around 0.3 nm, more than 10% of the total volume is accessible in the middle of the membrane. This value drops very fast, below 2%, going towards the denser packed lipid tails in region 3. Larger penetrants (>0.4

Downloaded¬13¬Nov¬2006¬to¬129.125.25.39.¬Redistribution¬subject¬to¬AIP¬license¬or¬copyright,¬see¬http://jcp.aip.org/jcp/copyright.jsp

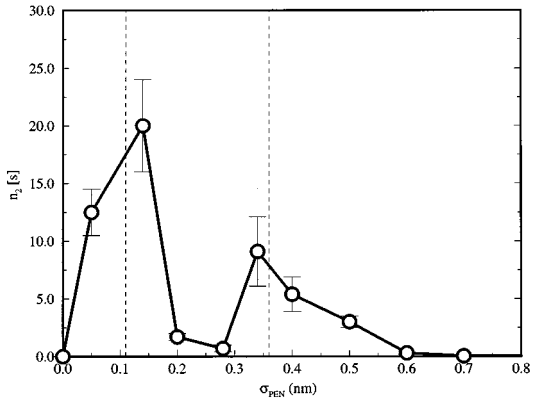

FIG. 2. Second moment of hole size distribution as function of penetrant size. Vertical lines indicate the percolation thresholds, estimated by fitting the curves locally to a Gaussian.

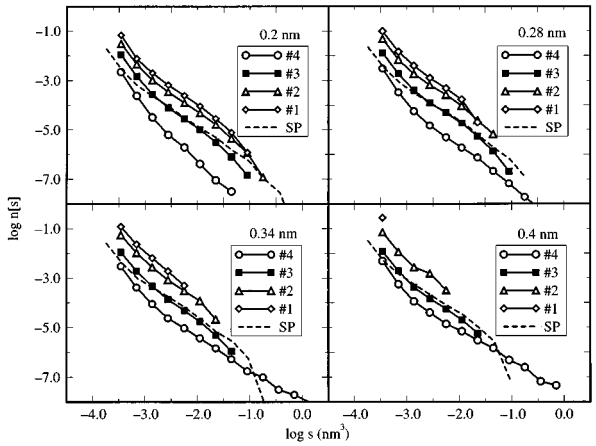

FIG. 3. Accessible hole size distribution for penetrants with a diameter of 0.2, 0.28, 0.34, and 0.4 nm, in the four membrane regions and in the soft polymer (SP) system. Total hole fractions are normalized to 1. Except for the largest holes, the statistical errors are negligibly small (see error discussion).

nm) have virtually no accessible free volume left in this region. The accessible free volume in the regions 1 and 2 is negligible for almost all penetrants; only for diameters smaller than 0.25 nm, the penetrant would fit into the holes in between of the water molecules. For a hard sphere of ~0.3 nm, the accessible free volume across a 1-glycerol monooleate (GMO)–water interface was calculated by Pohorille and Wilson.[12] These calculations show a decrease in accessible free volume at the interface, in agreement with our findings. The same authors further notice that the opposite, i.e., increase in accessible free volume, occurs at the water–dodecane interface. A recent comparative study[13] of a number of interfaces with varying degrees of hydrophobicity underlines this fundamental difference between more hydrophilic and more hydrophobic interfaces.

C. Percolation threshold

Since in general the free volume related properties of a system are quite different away from the percolation threshold than close to it (see theory section), it is interesting to determine the percolation thresholds in the lipid membrane system. In Fig. 2 we plot the second moment of the hole size distribution, from which we can estimate the percolation threshold. At the percolation threshold a maximum should occur. As we see from Fig. 2, we observe two maxima. This is due to the inhomogeneous free volume distribution in the membrane. The first maximum (at penetrant size $\sigma=0.36 \pm 0.02$ nm), arises from the lateral percolation of the free volume in region 4 of the membrane (this can be unambiguously determined by explicit evaluation of the size of the percolating cluster in both lateral, and perpendicular direction). If we compare Fig. 1, we see that for the percolating penetrant size the largest accessible free volume fraction p_c in region 4 is 0.06 ± 0.01. The second maximum ($\sigma=0.11 \pm 0.01$ nm) results from the percolation in the perpendicular direction. The bottle neck for percolation in the z direction is located in region 2. (This can be concluded from Fig. 1, which shows that for the percolating penetrant size the accessible free volume is lowest in region 2.) The lowest accessible free volume fraction p_c in this region is 0.06 ± 0.02 at the percolation threshold.

The soft polymer system also percolates at a free volume fraction of $p_c=0.06 \pm 0.005$. Apparently, the location of the percolation threshold is not very sensitive to the details of the system. This is further confirmed by the percolation threshold for a system of random overlapping spheres[8] (with diameters comparable to the atom sizes in the membrane systems), for which $p_c=0.06 \pm 0.005$.

Note that the calculated values of the percolation threshold are sensitive to the number of grid points. For larger grids, the percolation threshold becomes slightly smaller.[8] The above mentioned percolation thresholds are all based on similar grid sizes. The estimated percolation thresholds are in agreement with the estimations that are based on the criterium that 50% of the configurations percolate at the percolation threshold. The results based on the second moment of the hole size distribution turned out to be more accurate, however.

D. Hole size distribution

The distribution of free volume pockets (i.e., holes) in the membrane is considered to be of key importance to the diffusion process. We calculated the hole size distribution for different penetrant sizes, and for different regions in the membrane. The results are shown in Fig. 3. The hole size distribution of the soft polymer system is also included. Note that the distributions are normalized to the same total free volume, in order to make a comparison possible of the relative number density of different hole sizes.

The observed shapes of the curves in Fig. 3, are in general agreement with the results predicted by percolation theory. Power laws are observed for all membrane regions, over a varying range of hole sizes. Fitting of the curves to a power law over the range for which power law behavior is

Downloaded¬13¬Nov¬2006¬to¬129.125.25.39.¬Redistribution¬subject¬to¬AIP¬license¬or¬copyright,¬see¬http://jcp.aip.org/jcp/copyright.jsp

observed yields values in the range from 1.4 to 1.7. These values are close to the theoretical value of the scaling exponent θ, which is 1.5. Apparently the correlation length ξ is small, and Eq. (5) applies. This is to be expected, as we are far away from p_c in most regions.

For very small holes (i.e., smaller than the correlation length), a steeper size dependence is found. According to Eq. (4) the slopes in this region should be equal to $\tau=2.18$. The reason that we find larger values (~ 2.5) is probably due to finite size effects, which will dominate the true scaling behavior. (The same effects were found in the soft polymer simulation and in the case of percolation studies on random grids.[8]) Only in the case of region 4, for the smallest penetrant size, we find an exponent of 2.1, close to the theoretical value of $\tau=2.18$. In this case, the system is close to the percolation threshold, and Eq. (4) is valid over the whole range of hole sizes.

For very large holes, in most cases an exponential type of decay is observed, as predicted by Eq. (5). It should be mentioned that the statistical accuracy for the largest free volume clusters is quite poor, and therefore accurate fitting is not possible in this part.

Comparing the hole size distributions of the four different regions of the membrane, we observe that they behave rather differently, although normalized to the same total volume. Region 4 is characterized by the presence of relatively many large holes, which decay with a power law over a large range of hole sizes compared to the other regions. This follows from the fact that the accessible free volume in region 4 remains close to the percolation threshold even for the larger penetrants. Therefore, the exponential part of Eq. (5) will be close to one, even for larger holes. For the other regions, which are below the percolation threshold for all penetrant sizes, the exponential part will become important already at smaller hole sizes. In regions 1 and 2, for the largest penetrant sizes, the power law behavior is not observed at all.

The difference in hole size distributions between region 3 on one hand, and regions 1 and 2 on the other, is important. Although the empty free volume in theses three regions is not so different (see Fig. 1), there are relatively many more large holes in region 3 compared to regions 1 and 2. This effect can be understood, considering the relatively large accessible free volume in this region. With an accessible free volume fraction p that is closer to the percolation threshold p_c, Eq. (5) predicts an extended power law behavior, as is observed for region 3. Similar conclusions are also drawn from the cavity studies of Pratt and Pohorille,[14,15] who showed that liquid alkanes such as *n*-hexane and *n*-dodecane have a broader distribution of cavity sizes compared to liquid water. Although the empty free volume in water was slightly larger than in the alkane solvents, the accessible free volume for penetrants of substantial size is larger in the alkane solvents. Qualitatively these results match ours precisely.

If we compare the results of the lipid membrane with the results of the polymer membrane, then it is clear that the hole size distribution in region 3 resembles that of the polymer membrane very much, for all penetrant sizes. Only very large holes seem to be somewhat more probable in the polymer membrane with respect to region 3 of the lipid membrane.

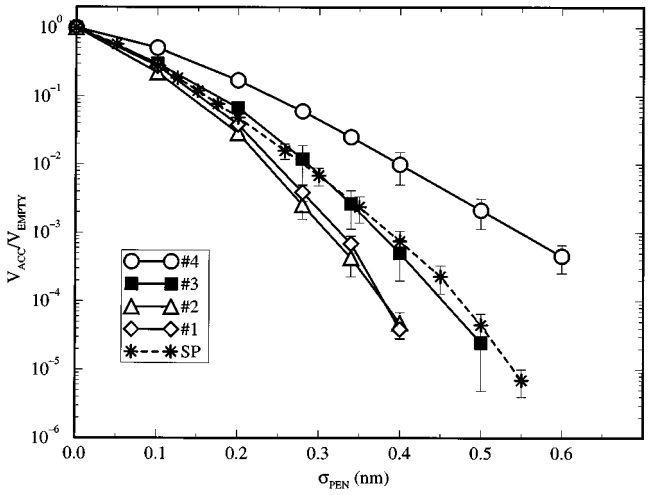

FIG. 4. Ratio of accessible and empty free volume as function of penetrant size, in the four membrane regions and in the soft polymer (SP). For small penetrant sizes, the statistical error is smaller than the figure marks.

E. Scaling of free volume

In order to further illustrate the resemblance between region 3 of the lipid membrane and the polymer membrane, we plotted in Fig. 4 the relative accessible free volume, i.e., the ratio of accessible free volume and empty free volume, against the penetrant size. As can be seen from this figure, the scaling behavior of the accessible free volume against penetrant size is different for each of the membrane regions. As anticipated, the scaling behavior of the accessible free volume in region 3 is quite similar to that of the polymer system.

Region 4 shows the highest relative accessible free volume compared to the other regions. This is a direct consequence of the fact that the accessible free volume in region 4 is closest to the percolation threshold. Closer to the percolation threshold, there are relatively more larger holes (see also Fig. 3). Therefore, the accessible free volume is expected to depend less strongly on penetrant size. This behavior is observed for all regions at small penetrant sizes. Region 4 shows this behavior over the whole range of penetrant sizes. As the regions become denser, the accessible free volume drops far below the percolation threshold. As a result, the larger holes become relatively rare and the curves become steeper.

Now it is an important question where the difference in scaling behavior of the accessible free volume in regions 1 and 2 vs region 3 originates. From the empty free volume distribution across the membrane (Fig. 1), we have seen that the empty free volume in region 3 is even smaller than in region 1. Nevertheless, the accessible free volume in region 3 is much larger, indicating that the free volume is relatively more clustered into larger holes. This is confirmed by the hole size distribution plots (Fig. 3). For clustered free volume, the accessibility will be clearly larger than for ran-

Downloaded¬13¬Nov¬2006¬to¬129.125.25.39.¬Redistribution¬subject¬to¬AIP¬license¬or¬copyright,¬see¬http://jcp.aip.org/jcp/copyright.jsp

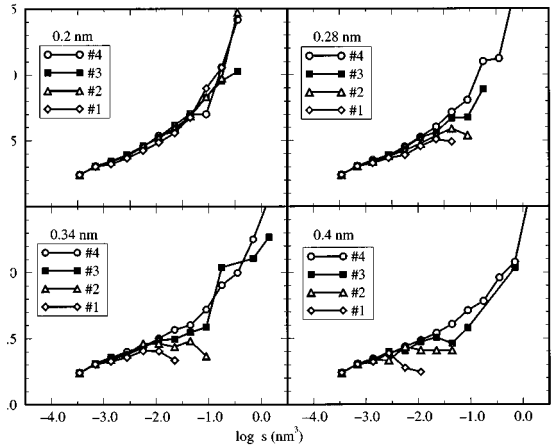

FIG. 5. Asphericity parameter for penetrants with a diameter of 0.2, 0.28, 0.34, and 0.4 nm, in the four membrane regions.

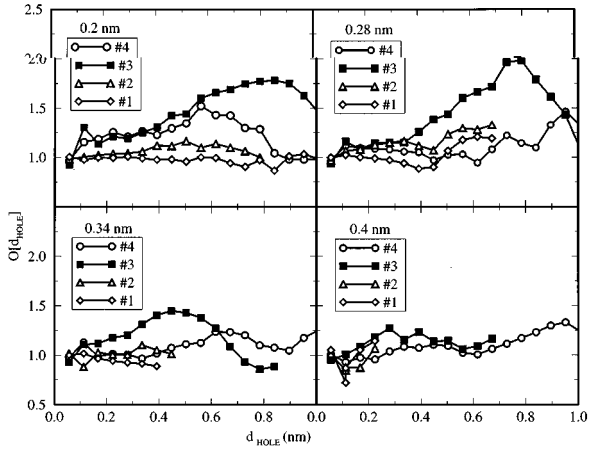

FIG. 6. Orientation parameter for penetrants with a diameter of 0.2, 0.28, 0.34, and 0.4 nm, in the four membrane regions.

domly distributed free volume. The origin of this additional connectivity of the free volume clusters in region 3 we attribute to the strong interaction between the lipid headgroups. As a result, the lipid tails in region 3 are more correlated (see the order parameter profile),[1] thereby increasing the correlation length of the free volume distribution also.

F. Asphericity parameter

Analysis of the asphericity parameter should give information about the shape of the penetrant-accessible holes. The results are plotted in Fig. 5, for various penetrant sizes, and in the four different regions of the membrane. Two observations are important. First, the increase of the sphericity parameter with increasing hole size, which indicates that larger holes are relatively more elongated and/or rougher than smaller ones. For small holes, the increase is more or less linear, with an asphericity parameter rising from $\sim$1.2 to $\sim$1.5. Assuming that for small holes the elongation dominates the roughening, and regarding them as perfect cylinders, the average ratio of long axis over short axis is calculated from Eq. (7) to increase from $\sim$3 to $\sim$10. The quantitative value of these numbers should be doubted, however, since the holes are not perfect cylinders.

For larger holes, the fractal character will become more and more important, and Eq. (8) is expected to dominate the scaling of the asphericity parameter. On the log scale of Fig. 5, this would imply an exponential increase of the asphericity parameter. This behavior is observed for the larger holes.

Qualitatively one can conclude that the larger holes are more elongated and/or more fractal than the smaller ones. Note that there is almost no difference between the different penetrant sizes, i.e., larger penetrants see similar hole shapes as smaller ones. One might expect that this is strange because larger penetrants fit into the larger holes only, which we observed to have a higher asphericity parameter. But this effect is apparently cancelled by the diminished possibility of larger penetrants to fit into holes which have more elongated shapes.

The second important observation, is that the asphericity parameter seems to decrease from region 4, via regions 3 and 2, to region 1. Although the data are quite noisy, this observation seems significant for all but the smallest holes. This means that in the water and headgroup regions the holes remain more spherical compared to the hole shapes in the membrane interior. Presumably, elongated holes are relatively stabilized in the membrane interior, due to the correlated nature of the lipid tails.

G. Orientation parameter

In order to characterize the aspherical shapes of the accessible free volume holes further, we also calculated the average orientation parameter of the holes with respect to the membrane normal. The result is shown in Fig. 6, again in different regions of the membrane, and as a function of penetrant size.

Although the noise is large in the orientation parameter curves, especially for the larger hole radii, it is clear that the largest anisotropy is found in region 3. The orientation parameter is larger than one, which means that the hole diameter in the z direction is, on average, larger than in the xy direction. The lipid order parameter profile[1] showed that the lipid tails are also preferentially oriented in the z direction, and that the largest ordering is found also in region 3. Therefore, it is of no surprise that the free volume in this region also shows the same behavior.

To the contrary, an almost complete isotropic orientation of free volume pockets is found in region 1. The isotropic distribution of the water molecules in this region clearly excludes the presence of anisotropically orientated free volume pockets.

Two other related observations can be made, although their statistical significance is doubtful. First, it seems that the orientation parameter gets smaller upon increasing penetrant size, and second, that the maximum of the orientation parameter distribution shifts towards smaller accessible holes for larger penetrants. This is most clear in region 3. If this is true, it would mean that the anisotropy of the holes is most

Downloaded¬13¬Nov¬2006¬to¬129.125.25.39.¬Redistribution¬subject¬to¬AIP¬license¬or¬copyright,¬see¬http://jcp.aip.org/jcp/copyright.jsp

pronounced for small holes only, i.e., holes that accommodate penetrants with sizes smaller than ~0.4 nm. Larger penetrants would therefore experience a much more isotropic distribution of holes.

V. DISCUSSION

A. Error discussion

The above calculated free volume properties of a lipid membrane, are based on the analysis of a rather short simulation (80 ps). Mean field MD simulations[16] of lipid membranes have indicated that correlation times of more than 1 ns exist (e.g., lipid wobbling motions), which are certainly not adequately sampled in the trajectory that we used for the free volume analysis. It is therefore necessary to make an estimation of the importance of these long-time lipid modes. In a number of subsequent simulations of our lipid membrane with similar force field parameters, used to study the permeation process of various small molecules, we have already reached a total simulation time of several nanoseconds. During these extended simulations we have tested a number of membrane properties upon the appearance of significant changes. All of the calculated properties, including lipid headgroup area, atomic distributions, and the accessible free volume distributions, remained rather close to those of the original simulation. Therefore, we can conclude that the trajectory analyzed in this paper has a distribution of conformations representative of the equilibrium state. To strengthen the confidence in the other free volume properties, we explicitly computed some hole size distributions averaged over the last 10 ps of the trajectory generated in the water permeation study.[2] The computed distributions agree very well with the ones presented in Fig. 3. Relatively large fluctuations are found for the largest hole sizes only, which is not surprising as they are exponentially rare.

Apparently, the redistribution of the free volume into smaller holes is determined by short time relaxation processes, such as position correlation times of water (in regions 1 and 2), or transitions of dihedral angles (in regions 3 and 4). The computed statistical errors are based on a division of the trajectory into separate intervals corresponding to these relaxation times. From our water permeation study,[2] we have deduced that in region 1 the water is on average only weakly bound to head group atoms, resulting in a correlation time of ~5 ps. In region 2 the hydration is stronger, with correlation times of 30 ps on average. Analysis of dihedral transition times[1] revealed lifetimes of ~30 ps and ~10 ps for regions 3 and 4, respectively. The statistical errors of regions 2 and 3 are therefore comparatively large. Again, we note that systematic errors might influence the properties of the largest clusters, and of the shape and orientation distributions (Figs. 5 and 6). These results should be interpreted with care. The statistical errors of the soft polymer simulation data are based on the relaxation time of the radius-of-gyration of the polymer chains, which was found to be ~75 ps (the length of the polymer trajectory was 500 ps).[3]

B. Free volume in the four regions

The results that we presented in this paper, show very clearly, that also in terms of free volume the lipid membrane is a complicated system. Due to the inhomogeneous and anisotropic nature of the bilayer, it cannot be approximated by any bulk phase. More realistically, the membrane can be described by the four region model. In terms of free volume properties, the regions can be characterized in the following way:

Regions 1 and 2: Small-molecule fluid. In terms of free volume properties, region 1 is not much different from bulk water and can be characterized as isotropic. Due to the small correlation length of the solvent atoms (i.e., mostly water in this region), the free volume is distributed in many small, spherical holes. Since the density is quite large, the accessible free volume for even the smallest penetrants is far below the percolation threshold. This implies that the hole size distribution is exponentially decaying and large free volume pockets are rare. Although region 2 is the most complicated region considering the variety of atoms found there, the free volume properties of this region are very similar to those in region 1. The accessible free volume is even less than in region 1 due to the high headgroup density. Such a drop in accessible free volume across a hydrophilic interface seems a common principle.

Region 3: Soft polymer. This is the most interesting region considering its free volume properties. Our analyses reveal that region 3 of the lipid membrane resembles a soft polymer in many respects. Not only the density and total free volume are similar, but also the accessible hole size distribution. Therefore, one can expect that the local environment for a penetrant in the soft polymer is very similar to that of region 3 of the membrane. This is illustrated by the similar scaling behavior of the accessible free volume (Fig. 4).

The reason why region 3 of the lipid membrane resembles a soft polymer, more than a bulk alkane, is the presence of a strong correlation between the chains. This correlation is in fact in both systems a consequence of the high density, coupled to the presence of solvent molecules which possess long range connectivity, e.g., chains. In the case of the lipid membrane, it is the strong interaction between the headgroups which causes the high density in region 3, and in the soft polymer system it is mainly a consequence of the relative low end group density. In both cases, the high density implies that the chains are packed more tightly together, therefore, will assume more correlated conformations.

As a result of these correlations, the hole size distributions are quite different from those in regions 1 and 2. Power law behavior is observed over a wider range of penetrant sizes. As a result, the scaling behavior of the free volume is less steep than is observed for regions 1 and 2. The anisotropic nature of region 3 is illustrated by the presence of relatively many aspherical holes, which are preferentially oriented along the membrane normal. This is a direct consequence of the alignment of the lipid tails in this region.

Region 4: Fluid decane. Due to the high end group density in this region, it has a large amount of accessible free

Downloaded¬13¬Nov¬2006¬to¬129.125.25.39.¬Redistribution¬subject¬to¬AIP¬license¬or¬copyright,¬see¬http://jcp.aip.org/jcp/copyright.jsp

volume, which is distributed much more isotropically compared to region 3. Due to the low density, the accessible free volume fraction for small penetrants remains close to the percolation threshold. Therefore, the free volume is distributed in relatively large holes, and even large penetrants (e.g., with diameters of 0.5 nm) could fit locally into this region without disturbing the lipid conformations. The isotropic nature, the large end group density and the large free volume fraction of this region validate the assumption that it resembles a low density alkane fluid, like decane. Analysis of the free volume properties of bulk decane simulation would be required to verify the resemblance, however.

C. Free volume and permeation

Knowing the free volume properties in the four membrane regions, we will now anticipate on its effect on the permeation process of small molecules. First of all, it appears that a homogeneous solubility-diffusion model is not likely to be a good model for describing the permeation process across a lipid membrane. In such a model, which is often applied for lipid membranes, the membrane is considered as a homogeneous bulk phase. The permeation process is then regarded as a three-step process: solvation of the penetrant from the water phase into the membrane phase, diffusion across the membrane, the dissolvation into the water phase again. With the free volume results in mind, we expect that both the diffusion step and the solvation/dissolvation step are oversimplified by a homogeneous description.

The diffusional part of the permeation process will certainly reflect the inhomogeneous nature of the free volume properties in the membrane. Our analysis shows that the four membrane regions that we distinguished show distinct behavior. Whether the total diffusion rate across the membrane will resemble a soft polymer, a bulk alkane or a high density fluid will depend on the location of the rate limiting step. This can be different for different kind of penetrants, however. The experimentally observed resemblance between the diffusion process of small penetrants across lipid membranes and soft polymers[4,5] can be understood if the rate limiting step is located in region 3 for most penetrants.

Our results further show that the free volume properties in the lipid membrane depend very much on the size of the penetrants. Not only decreases the amount of accessible free volume for larger penetrants, which is quite obvious, but also the relative number of small and large holes varies. One could therefore expect different diffusional mechanisms for different penetrants. Therefore, quantitative predictions of diffusion rates that are based on free volume properties of the membrane only, without taking into account the penetrant properties explicitly, are difficult. Both the difference between each of the membrane regions and the dependence of free volume properties on penetrant size makes the application of any general free volume theory useless. For instance, the simple free volume theory of Cohen and Turnbull[17] generally applies to systems for which the hole size distribution is exponentially decaying. For the membrane, this only holds for regions 1 and 2. Regions 3 and 4 only show exponentially decaying hole sizes for large penetrant molecules. More sophisticated free volume based diffusion theories[18,19] are applied in the soft polymer field, but quantitative predictions of diffusion rates are also in these cases difficult. Either the assumptions are still too crude or the theory becomes too specific, involving many system-dependent parameters. Not only static free volume properties, but also dynamic ones are required for an accurate description. Transfer of free volume theories with quantitative predictive power to a much more complicated lipid membrane is therefore not possible.

From regression analysis of permeation data,[5] it has been concluded that the solvation part of the permeation process is not very different from solvation into an apolar solvent like hexadecane. But from our free volume analysis one would expect a somewhat more complicated picture. The inhomogeneous nature of the membrane interior is not likely to result in a constant excess free energy of solvation. From the free volume analysis one would expect that the entropy part of solvation is favored in low-density region 4 much more than in high-density region 3. For the enthalpy part of solvation, the opposite might be true. Especially for elongated molecules, the penetrant–lipid interactions in the anisotropic region 3 may result in a relative stabilization. The average effect of regions 3 and 4, however, could result in a total solvation free energy which is not very different from solvation into hexadecane.

As is obvious from the preceding discussion, the lipid membrane is rather complicated in terms of free volume. General predictions of the permeation process based on free volume only are difficult, and more explicit studies of penetrant–lipid systems will be needed. In our extended studies[2,11,20] of other penetrant molecules we indeed see that the permeation process of small penetrants can be modeled realistically in an inhomogeneous solubility-diffusion model, in which both the solubility and the diffusion are considered as function of membrane position, and not as step functions. We will show that the different free volume properties of the four membrane regions have large consequences for the permeation process of penetrants that differ in size, hydrophobicity, and shape.

VI. CONCLUSION

The analysis of various free volume properties of a lipid membrane have reaffirmed that the lipid membrane is both inhomogeneous and anisotropic. Splitting the membrane in different regions, the free volume properties resemble those of a small-molecule fluid in the interfacial regions, a soft polymer in the high density part of the lipid tail region, and fluid decane in the middle of the membrane. Assuming that the permeation process of small molecules is strongly related to the free volume properties, qualitative predictions can be made for diffusion and solubility properties of a variety of penetrants. Considering the strong dependence of free volume properties on penetrant size, and the difference in free volume properties between the different membrane regions, the existence of a simple quantitative relationship between permeation rates and free volume properties can be ruled out.

Downloaded¬13¬Nov¬2006¬to¬129.125.25.39.¬Redistribution¬subject¬to¬AIP¬license¬or¬copyright,¬see¬http://jcp.aip.org/jcp/copyright.jsp

ACKNOWLEDGMENT

This work was supported by the Foundation for Biophysics and the Foundation for National Computer Facilities under the auspices of the Netherlands Organization for Pure Research, NWO.

[1] E. Egberts, S. J. Marrink, and H. J. C. Berendsen, Eur. Biophys. J. **22**, 423 (1994).
[2] S. J. Marrink and H. J. C. Berendsen, J. Phys. Chem. **98**, 4155 (1994).
[3] R. M. Sok and H. J. C. Berendsen (unpublished).
[4] W. R. Lieb and W. D. Stein, Curr. Top. Membr. Transp. **2**, 1 (1971).
[5] A. Walter and J. J. Gutknecht, Membr. Biol. **90**, 207 (1986).
[6] D. Stauffer and A. Aharony, *Introduction to Percolation Theory* (Taylor & Francis, London, 1992).
[7] W. F. van Gunsteren and H. J. C. Berendsen, *Groningen Molecular Simulation (GROMOS)*; software package, Biomos, Nijenborgh 4, 9747 AG Groningen, The Netherlands.
[8] R. M. Sok, S. J. Marrink, and H. J. C. Berendsen, J. Pol. Sci. (submitted).
[9] R. M. Sok and S. J. Marrink, *PERCOBIN*, free obtainable software package, University of Groningen, 1992.
[10] A. Bondi, J. Phys. Chem. **58**, 929 (1954).
[11] S. J. Marrink, Thesis, University of Groningen, 1994.
[12] A. Pohorille and M. A. Wilson, J. Mol. Struct. **284**, 271 (1993).
[13] A. R. van Buuren, S. J. Marrink, and H. J. C. Berendsen, Colloids and Surfaces A: Phys. Eng. Aspects **102**, 143 (1995).
[14] A. Pohorille and L. R. Pratt, J. Am. Chem. Soc. **112**, 5066 (1990).
[15] L. R. Pratt and A. Pohorille, Proc. Natl. Acad. Sci. USA **89**, 2995 (1992).
[16] H. De Loof, S. C, Harvey, J. P. Segrest, and R. W. Pastor, Biochemistry **30**, 2099 (1991).
[17] M. H. Cohen and D. J. Turnbull, Chem. Phys. **31**, 1164 (1959).
[18] H. Fujita, Fortschr. Hochpolym. Forsch. **3**, 1 (1961).
[19] J. S. Vrentas and J. L. Duda, Macromolecules **9**, 785 (1976).
[20] S. J. Marrink and H. J. C. Berendsen, J. Phys. Chem. (submitted).

Downloaded¬13¬Nov¬2006¬to¬129.125.25.39.¬Redistribution¬subject¬to¬AIP¬license¬or¬copyright,¬see¬http://jcp.aip.org/jcp/copyright.jsp